

Jadwiga Zalewska, Jan Kaczmarczyk, Grażyna Łykowska
Oil and Gas Institute, Krakow

Use of X-ray computed microtomography for analysis of drill cores

Introduction

Laboratory measurements of drill cores are being performed in Oil and Gas Institute for purposes of oil industry, in order to determine petrophysical features in aspect of their reservoir properties and pore space connectivity, that enable migration of reservoir media.

Clastic reservoir rocks having diversified structure and texture, as well as featuring various cement and saturation of pores space, have been analysed until now with method of thin slices microscopic examination in polarised light. Now it is possible to “look into rock interior” with micro-CT method. Use of this method enables determination of rock porosity, measuring length of pore throats, evaluation of their tortuosity, observation of water or oil penetration into rock, with visualisation and analysis of wetting process. This method also enables visualisation of fractures and makes measurement of their aperture and width pos-

sible, which is of particular importance first of all when it comes to deal with reservoir rocks of low porosity and permeability, where production of hydrocarbons depends mainly on number of open fractures. The information is necessary in complex interpretation of well log geophysics data, and characteristic values of these properties are also used as input data for various modelling of rock pore space impact on values of measurable physical parameters (e.g. density, electrical resistivity, propagation velocity of acoustic wave, etc.).

It will also have fundamental importance in analysis of fissure systems in shale rocks. Presence of such type fractures in shale rocks may have essential impact on shale gas production method. It may also ensure its cost-effective production, particularly for reservoirs deposited on big depths.

Methodology of examination performance

The study presents results obtained with use of Benchtop 160 CT X-ray microtomograph. Measurements were completed at 110 kV lamp voltage and 73 μ A current. Scanning duration amounted to approx. 3 hours for single sample.

Cylindrical samples 10 mm diameter and 20 mm length were subjected to examination, as twenty-two fold magnification was possible during measurement for samples of such dimensions, which directly translated on obtaining of good resolution for acquired images at 6 μ m level.

The immediate result of microtomograph operation are projections that are representation of 3D object onto 2D matrix. Each such image contains information on radiation intensity attenuation inside a three-dimensional object.

Only after processing (reconstruction) of these projections, spatial image of the sample is possible to obtain. The images were reconstructed with use of CT-Pro (X-Tek) software package.

Detailed descriptions of micro-CT theory and its applications for rock porous systems can be found in numerous publications [e.g. 1, 2, 3, 4].

Tomographic porosity was calculated as number of voxels belonging to pore layer to total number of image voxels ratio.

Spatial visualisation of whole rock original structure was done, next porosity distribution analysis performed, which was based on division of pore network on subgroups.

Each subgroup constitutes set of interconnected pores, but not communicating with other subgroups. The subgroups were divided into classes by their volume (Tab. 1). Quantitative analysis of the subgroups is presented in form of two graphs. The first one is the graph of subgroups size in individual volume classes, and shows the extent to which specific class is divided. The second graph presents distribution of pore network volume classes. It created base enabling approximate statistical analysis of pore space.

Fractures were discerned in individual samples, and their apertures and widths have been measured. Inclination angle of the fractures, as well as distance between neighbouring fractures have also been measured. Besides

measurement of fractures lamination angle, also measurement of fractures volume percentage in rock sample is possible, and – which is most important – accurate fracture width measurement in arbitrary place.

Then tortuosity of pore throats for all interconnected pores present in sample was calculated. Three-dimensional nature of micro-CT examination enabled tortuosity measurement in three directions perpendicular to each other: X, Y and Z, providing information on possible anisotropy in pore space distribution, as well as fluid flow paths within reservoir rocks. Tortuosity of all potential flow paths was determined only when connections of pore throats between two opposite sides of examined sample were present.

Table 1. Method of pore volume classes determination

Pore volume [voxel]	1÷9	10÷99	100÷999	1000÷9999	10 000÷99 999	>100 000
Pore volume [μm^3]	$2 \cdot 10^2 \div 2 \cdot 10^3$	$2 \cdot 10^3 \div 2 \cdot 10^4$	$2 \cdot 10^4 \div 2 \cdot 10^5$	$2 \cdot 10^5 \div 2 \cdot 10^6$	$2 \cdot 10^6 \div 2 \cdot 10^7$	$>2 \cdot 10^7$
Class	I	II	III	IV	V	VI
Colour	yellow	blue	red	green	white	violet

Results of examinations

The study presents results of micro-CT examinations of internal structure for 5 carbonate rock samples originating from various boreholes. The carbonates were represented by samples No. 8761 (Z-2K borehole) and 9428 (B-6 borehole), dolomitic limestone – 9421 (B-5 borehole) and dolomite – 8617 (GR-2 borehole) and 9439 (B-8 borehole).

Additionally auxiliary measurements were performed for all analysed samples, which include: total porosity (“helium” method), absolute porosity (gas method with nitrogen use), microscopic observations (polarisation microscope – thin slices) and mineral composition (X-ray diffraction).

8761 sample is limestone containing 96% of calcite in its composition. It has been found on the grounds of

microscopic analysis, that this is bioclastic wackestone (according to Dunham classification). Spatial distribution of pores in this sample with division on volume classes was shown on Fig. 1. Pores create subgroups of sizes belonging to I to VI classes. There is fracture present in the sample, constituting pore of VI volume class and occupying majority of this sample pore space (Fig. 2). Fracture system was observed, from which two measured fractures had 9.22 μm up to 14.87 μm width and 2,74° and 2,93° aperture angles.

The biggest fracture in the sample is surrounded by numerous smaller pores, from which pores of II and III class contribute significantly to pore space volume. The fracture itself constitutes approx. 60% of pore space vol-

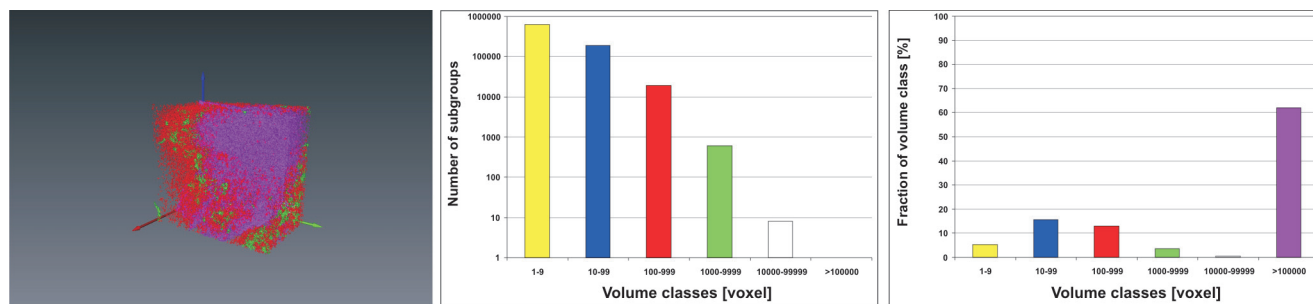


Fig. 1. Microtomographic analysis of 8761 sample (porosity 11.6%)

a) spatial pore distribution with division on classes (III–VI classes), b) quantitative fraction of pore classes, c) volumetric fraction of pore classes

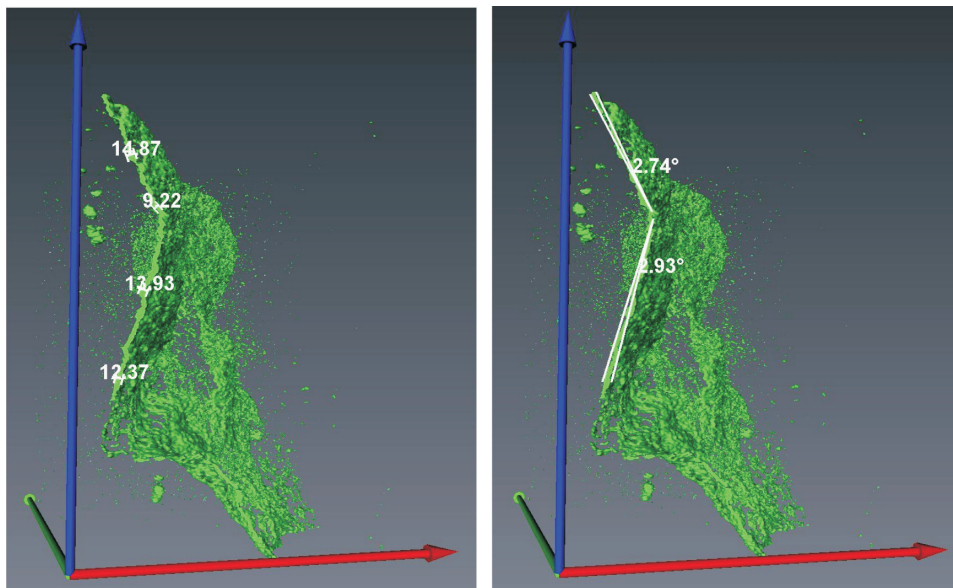


Fig. 2. Microtomographic image of section through 8761 sample fracture

X axis – red colour, *Y* axis – green colour, *Z* axis – blue colour

Table 2. Results of pore throats geometrical tortuosity measurement with micro-CT method – 8161 sample

Direction of tortuosity analysis	Absolute number of voxels from tunnel	Relative number of voxels from tunnel	Average tortuosity	Maximum tortuosity	Minimum tortuosity	Standard deviation from average value
<i>X</i>	23318	0.04	1.47	2.07	1.26	0.18
<i>Y</i>	28409	0.08	1.27	2.26	1.19	0.11
<i>Z</i>	18700	0.05	1.25	1.58	1.15	0.06

ume. It provides connections (of shape deviating from straight line) between opposite sides of the sample in all directions. Average tortuosity of the fracture in *X* direction is higher than in *Y* and *Z* directions. Connections in *Z* direction are more uniform than in *X* direction (Tab. 2).

9428 sample is a limestone with dominating fraction of calcite (96%), developed mainly in form of sparite. Fig. 3 illustrates 3D distribution of pores in this sample, while Fig. 4 presents the fracture which occupies approx. 70% of the whole pore space volume. Clearly developed fracture

has width from 20.62 μm up to 34.00 μm and aperture angle 2.09° or 3.67° – depending on measurement plane.

The fracture present in 9428 sample ensures connections between opposite sides of the sample in all directions. The connections in *X* direction are more rectilinear, while in *Z* direction are more complex (Tab. 3). Pores of I–V classes can be also observed besides the fracture, but only those of II–IV classes contribute significantly to pore space volume.

Presence of this fracture, as the only one from those examined, was confirmed also with microscopic examinations.

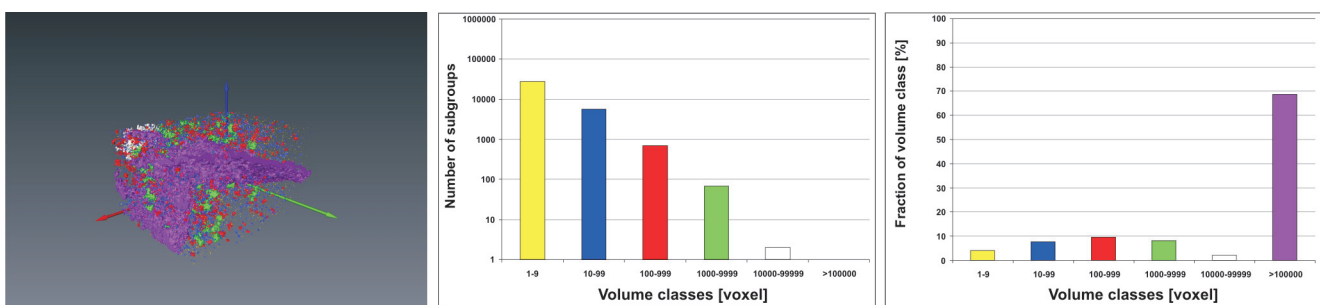


Fig. 3. Microtomographic analysis of 9428 sample (porosity 7.0%)

a) spatial pore distribution with division on classes, b) quantitative fraction of pore classes, c) volumetric fraction of pore classes

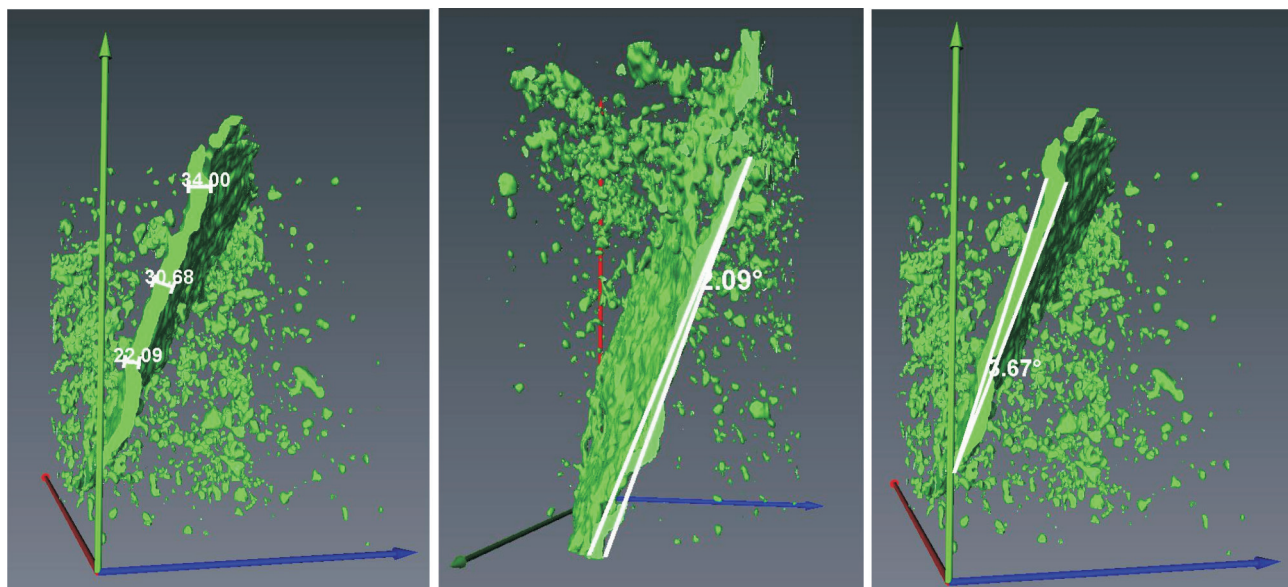


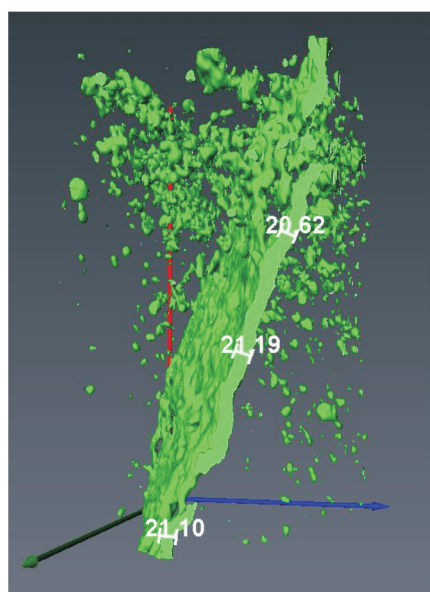
Fig. 4. Microtomographic image of section through 9428 sample fracture

X axis – red colour, Y axis – green colour, Z axis – blue colour

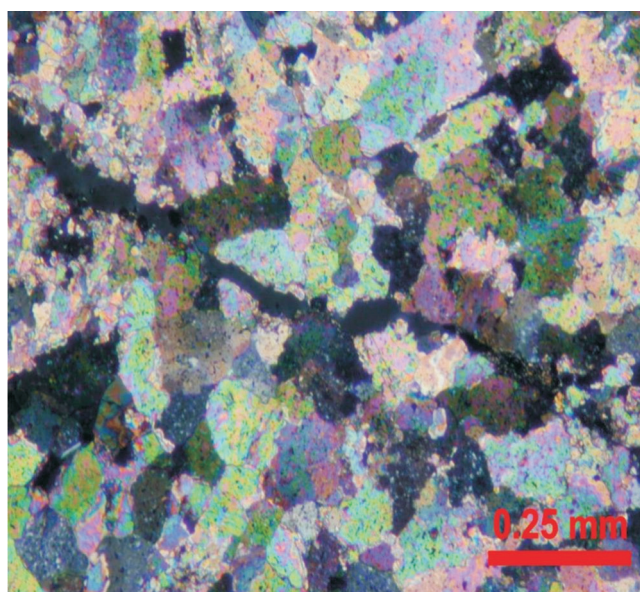
Table 3. Results of pore throats geometrical tortuosity measurement with micro-CT method – 9428 sample

Direction of tortuosity analysis	Absolute number of voxels from tunnel	Relative number of voxels from tunnel	Average tortuosity	Maximum tortuosity	Minimum tortuosity	Standard deviation from average value
X	6838	0.10	1.39	1.72	1.10	0.20
Y	4491	0.05	1.61	2.02	1.46	0.14
Z	2887	0.02	1.82	2.41	1.56	0.17

Micro-CT image



Microscopic image



Comparison of microtomographic image with microscopic image for 9428 sample

9421 sample is dolomitic limestone containing 88% of calcite and 11% of dolomite. Originally it could be packstone (according to Dunham classification). Limited

compaction traces indicate very early dolomitic cementation. The rock exhibits poor diagenesis.

Microtomographic analysis of this sample revealed

a **fracture**, which occupies approximately 85% of whole pore space volume. The remaining part of this space is composed mainly from V class pores, and pores of the remaining classes do not contribute significantly to pore space volume (Fig. 5).

Presented three-dimensional images show single, wide fracture, which aperture in the widest point reaches 40.4° , while it is much lower in its second segment, and determined as 8.78° . Width of the fracture ranges from $14.42 \mu\text{m}$ up to $200.00 \mu\text{m}$ (Fig. 6). Examined fracture is divided

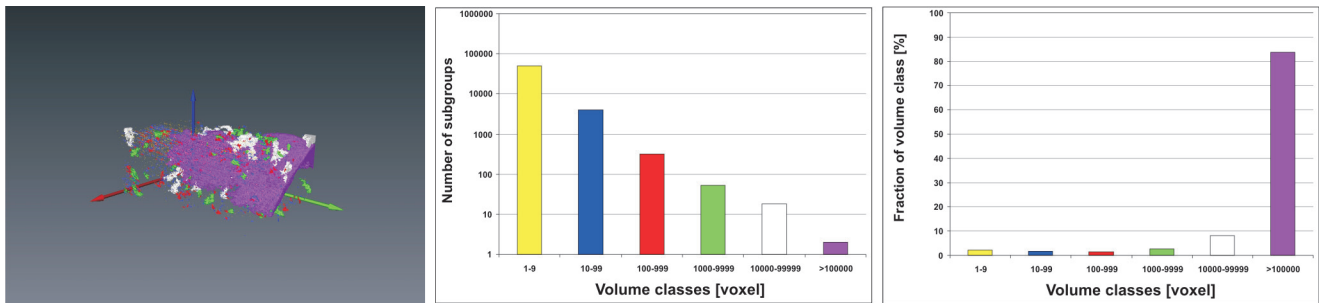


Fig. 5. Microtomographic analysis of 9421 sample (porosity 6.8%)

a) spatial pore distribution with division on classes, b) quantitative fraction of pore classes, c) volumetric fraction of pore classes

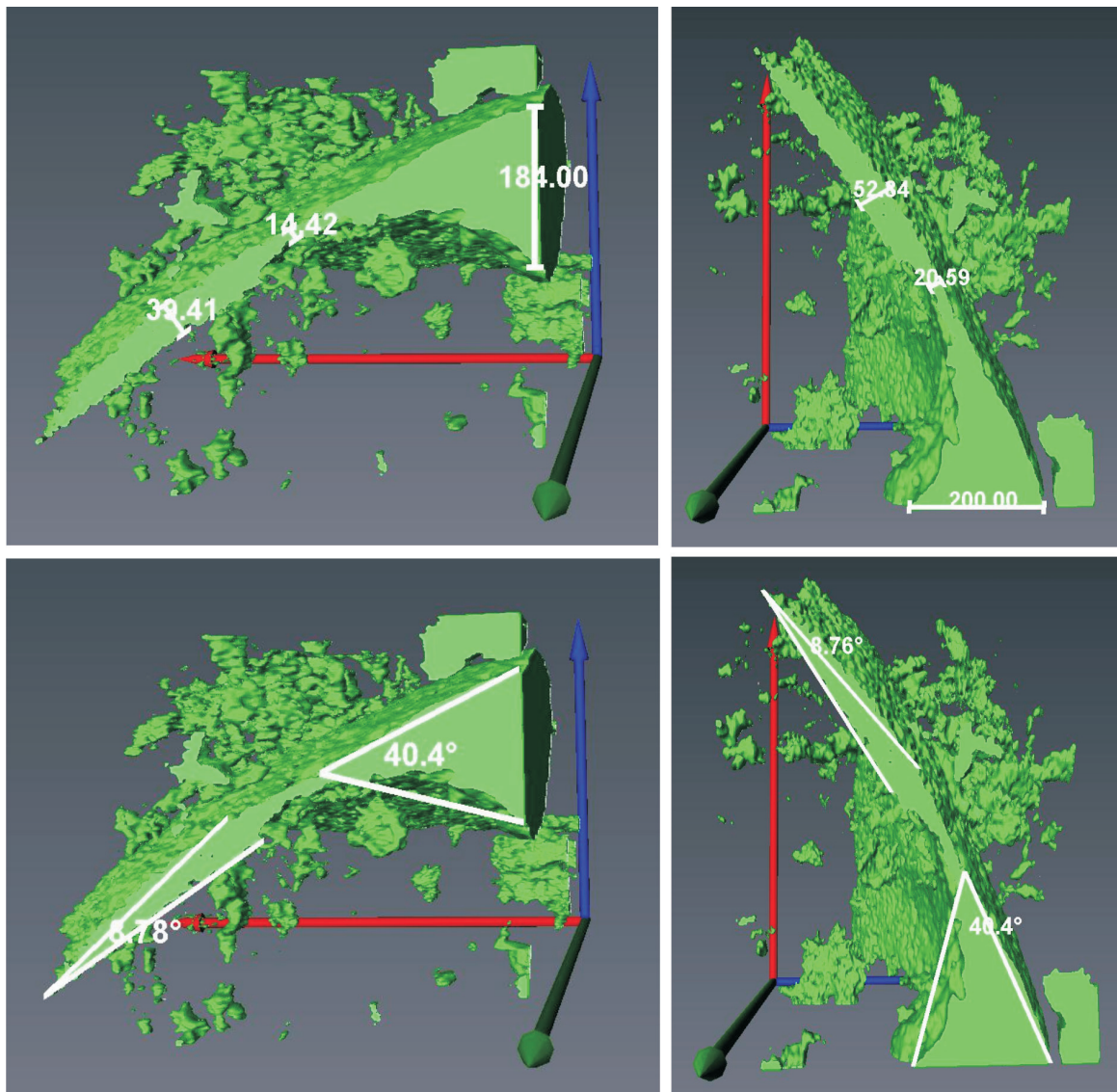


Fig. 6. Microtomographic image of section through 9421 sample fracture

X axis – red colour, Y axis – green colour, Z axis – blue colour

into several objects, and this is why it does not provide connections between opposite walls of the sample.

8617 sample represents fine-grain and diagenetic rock, in which mainly dolomite is present, creating dolosparite. Quartz grains and opaque minerals are dispersed over whole rock. The main mineral component is dolomite (90%), with calcite (4%) and quartz (5%) being also present. It results from microtomographic analysis that fracture is present in the sample, occupying approximately 50% of pore space volume, which was illustrated on Fig. 7. Many pores of lower volumes are present in the sample besides the fracture, from which contribution of II–III class pores is of significance.

Two fractures are present on images presented above. One fracture has width ranging from 11.05 μm up to 13.34 μm and aperture angle 1.22°, while width of the second fracture ranges from 14.04 μm up to 46.04 μm (Fig. 8).

The fracture is divided into several objects, nonetheless it provides connections between opposite sides of the sample in all directions. The connections are closest to rectilinear ones in *X* direction, while most complex and most diversified in *Z* direction. The connections in *Y* direction locate themselves, as regards shape, between connections in the remaining directions, and are uniform to relatively highest degree (Tab. 4).

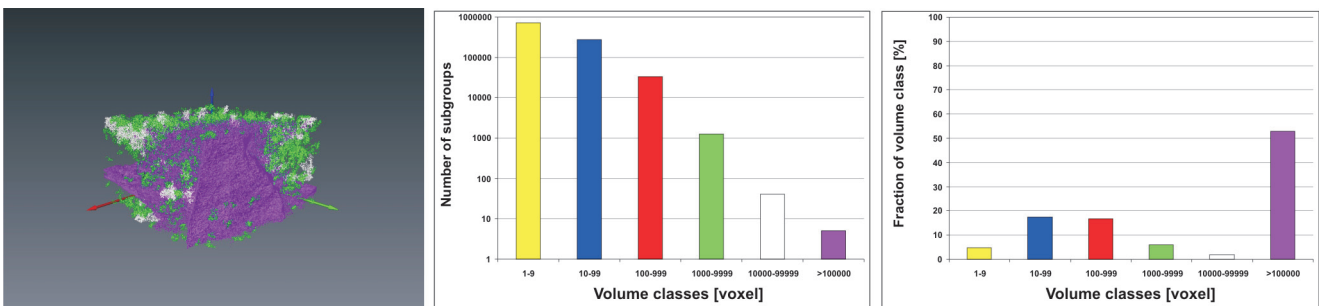


Fig. 7. Microtomographic analysis of 8617 sample (porosity 11.7%)

a) spatial pore distribution with division on classes, b) quantitative fraction of pore classes, c) volumetric fraction of pore classes

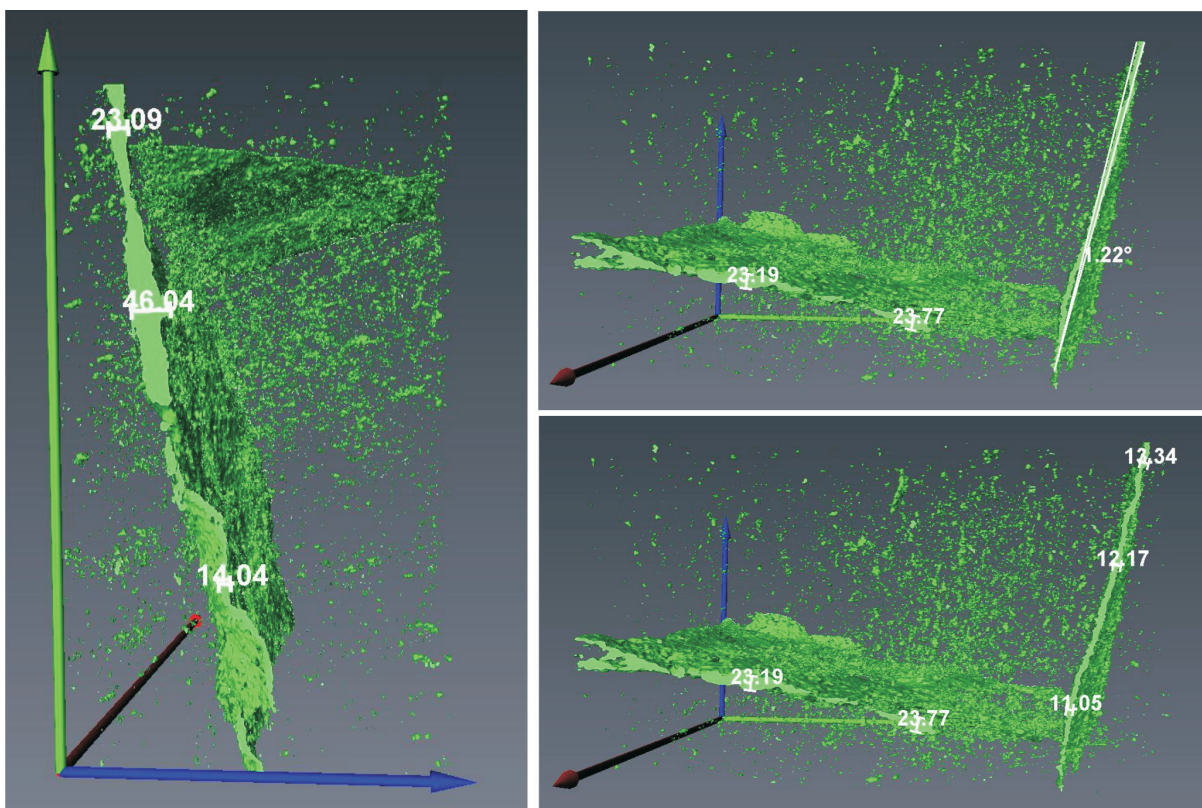


Fig. 8. Microtomographic image of section through 8617 sample fracture

X axis – red colour, *Y* axis – green colour, *Z* axis – blue colour

Table 4. Results of pore throats geometrical tortuosity measurement with micro-CT method – 8617 sample

Direction of tortuosity analysis	Absolute number of voxels from tunnel	Relative number of voxels from tunnel	Average tortuosity	Maximum tortuosity	Minimum tortuosity	Standard deviation from average value
X	16278	0.04	1.24	1.82	1.02	0.24
Y	24115	0.05	1.34	2.06	1.07	0.16
Z	16039	0.02	1.64	2.98	1.06	0.32

9439 sample represents anhydrite dolomite, which originally was packstone according to Dunham classification. It results from microtomographic analysis (Fig. 9) that the sample is characterised with VI volume class presence, which is modal value. This is connected with presence of fracture, which constitutes over 90% of whole pore space volume. Pores of the remaining classes do

not contribute significantly to pore network volume. The fracture is divided into approximately 10 objects.

In the separated space of microtomographic image, a fracture of width ranging from 23.71 μm up to 37.58 μm was shown (Fig. 10).

The fractures ensure connections between opposite walls of the sample in all primary directions (Tab. 5). These

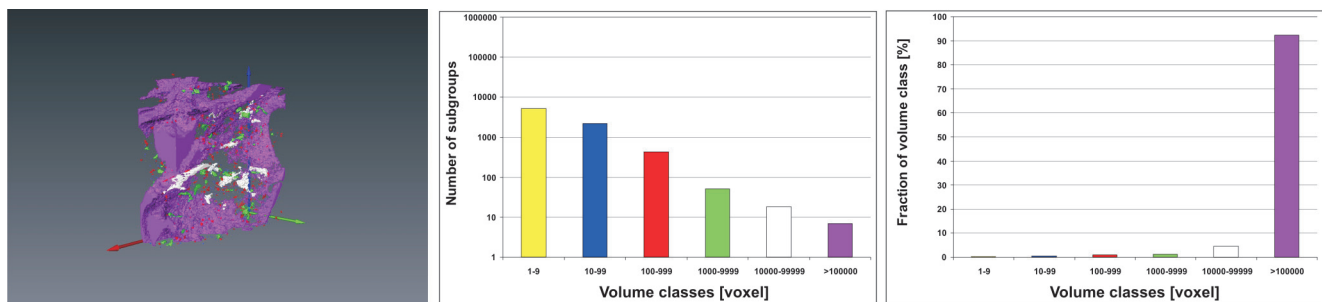


Fig. 9. Microtomographic analysis of 9439 sample (porosity 7.0%)

a) spatial pore distribution with division on classes, b) quantitative fraction of pore classes, c) volumetric fraction of pore classes

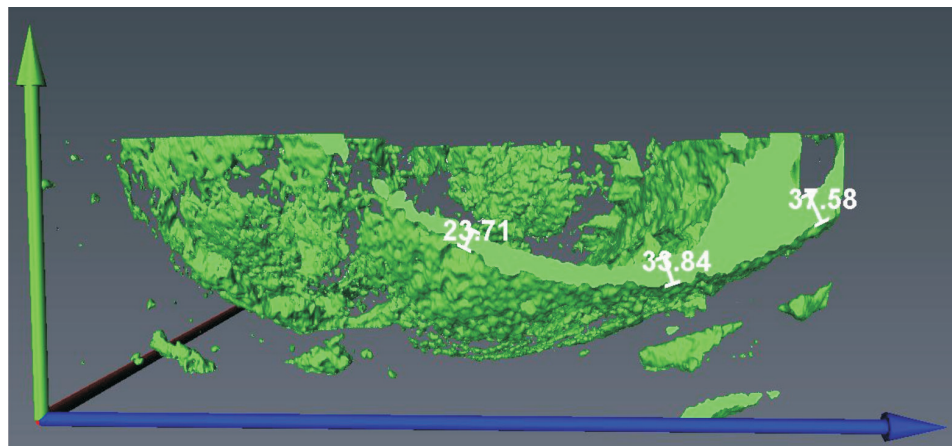


Fig. 10. Microtomographic image of section through 9439 sample fracture

X axis – red colour, Y axis – green colour, Z axis – blue colour

Table 5. Results of pore throats geometrical tortuosity measurement with micro-CT method – 9439 sample

Direction of tortuosity analysis	Absolute number of voxels from tunnel	Relative number of voxels from tunnel	Average tortuosity	Maximum tortuosity	Minimum tortuosity	Standard deviation from average value
X	1299	0.01	1.14	1.16	1.13	0.01
Y	14148	0.02	2.05	2.87	1.28	0.31
Z	13029	0.06	1.27	1.39	1.17	0.06

connections are closest to rectilinear ones in X direction, while complex to the highest degree in Y direction. Similarly uniformity of paths is changing in all directions. The

entry area to pore system in X direction is approximately 10 times lesser than in Y and Z directions. Research shown diversity of fractures shape in examined samples.

Summary

Completed analyses indicate significant usefulness of X-ray microtomography for determination of reservoir and filtration properties of rocks. They enable qualitative and quantitative analysis of porosity distribution with consideration given to pore throat connections between them, as well as distinguishing of fractures and their characterisation. Such examinations enable analysis of rock pore network parameters within broad examination spectrum, moreover, they are based rather on averaged than on single measurement of porosity.

General advantage of micro-CT method, as compared to microscopic method, is possibility of fracture visualisation in three-dimensional space and documentation of

these images with particular consideration given to fracture runs within sample, and possibility of their aperture changes determination. Three-dimensional analysis and accurate determination of aperture enable, on condition of proper orientation of cores, determination of fracture permeability tensor.

Analysis of fractures is of particular importance in case of cores originating from shale-gas type reservoirs. Presence of patent microfissures' natural network in shale rock provides non-zero permeability in such type reservoirs. This means spontaneous production from such reservoir and increased possibilities of production intensification.

Artykuł nadesłano do Redakcji 11.04.2011 r. Przyjęto do druku 13.04.2011 r.

Recenzent: prof. dr hab. inż. Andrzej Kostecki

References

- [1] Rivers M.: *Tutorial Introduction to X-ray Computed Microtomography Data Processing*. University of Chicago, 1999.
- [2] Van Geet M., Lagrou D., Swennen R.: *Porosity measurements of sedimentary rocks by means of microfocus X-ray computed tomography (μ CT)*. Geological Society, London, Special Publications, vol. 215, 51–60, 2003.
- [3] Van Geet M., Swennen R., Wevers M.: *Quantitative analysis of reservoir rocks by microfocus X-ray computerised tomography*. *Sedimentary Geology*, 132, 25–36, 2000.
- [4] Wellington S.L., Vinegar H.J.: *X-ray Computerized Tomography*. *Journal of Petroleum Technology*, 39, 885–898, 1987.



Mgr Jan KACZMARCZYK – absolwent Wydziału Chemii Uniwersytetu Jagiellońskiego na specjalności: Kataliza i chemia powierzchni ciała stałego. Pracuje w Zakładzie Geofizyki Wiertniczej Instytutu Nafty i Gazu w Krakowie. Zajmuje się badaniami metodą mikrotomografii rentgenowskiej, komputerowym przetwarzaniem i analizą obrazu oraz symulacjami numerycznymi.



Mgr inż. Jadwiga ZALEWSKA – geolog, absolwentka AGH. Kierownik Zakładu Geofizyki Wiertniczej Instytutu Nafty i Gazu w Krakowie. Realizuje prace badawcze w zakresie laboratoryjnych pomiarów parametrów rdzeni i płuczek wiertniczych pod kątem ilościowej interpretacji profilowań geofizycznych. Autorka 132 publikacji.



Mgr inż. Grażyna ŁYKOWSKA – absolwentka Wydziału Inżynierii i Technologii Chemicznej Politechniki Krakowskiej, na kierunku Inżynieria Chemiczna i Procesowa, specjalizacji Inżynieria Procesów Technologicznych. Pracownik Zakładu Geofizyki Wiertniczej INiG w Krakowie. Zajmuje się analizą rentgenowską składu mineralnego skał oraz badaniem ich właściwości petrofizycznych.